

Formulation of Highly Soluble Poly(ethylene glycol)-Peptide DNA Condensates

KAI Y. KWOK, DONALD L. MCKENZIE, DAVID L. EVERS, AND KEVIN G. RICE*

Contribution from *Divisions of Pharmaceutics and Medicinal Chemistry, College of Pharmacy, University of Michigan, Ann Arbor, Michigan 48109-1065.*

Received March 4, 1999. Accepted for publication July 19, 1999.

Abstract □ Two poly(ethylene glycol) (PEG)-peptides were synthesized and tested for their ability to bind to plasmid DNA and form soluble DNA condensates with reduced spontaneous gene expression. PEG-vinyl sulfone or PEG-orthopyridyl disulfide were reacted with the sulfhydryl of Cys-Trp-Lys₁₈ (CWK₁₈) resulting in the formation of nonreducible (PEG-VS-CWK₁₈) and reducible (PEG-SS-CWK₁₈) PEG-peptides. Both PEG-peptides were prepared on a micromole scale, purified by RP-HPLC in >80% yield, and characterized by ¹H NMR and MALDI-TOF. PEG-peptides bound to plasmid DNA with an apparent affinity that was equivalent to alkylated (Alk)CWK₁₈, resulting in DNA condensates with a mean diameter of 80–90 nm and ζ (zeta) potential of +10 mV. The particle size of PEG-peptide DNA condensates was constant throughout the DNA concentration range of 0.05–2 mg/mL, indicating these to be approximately 20-fold more soluble than AlkCWK₁₈ DNA condensates. The spontaneous gene transfer to HepG2 cells mediated by PEG-VS-CWK₁₈ DNA condensates was over two orders of magnitude lower than PEG-SS-CWK₁₈ DNA condensates and three orders of magnitude lower than AlkCWK₁₈ DNA condensates. PEG-VS-CWK₁₈ efficiently blocked *in vitro* gene transfer by reducing cell uptake. The results indicate that a high loading density of PEG on DNA is necessary to achieve highly soluble DNA condensates that reduce spontaneous *in vitro* gene transfer by blocking nonspecific uptake by HepG2 cells. These two properties are important for developing targeted gene delivery systems to be used *in vivo*.

Introduction

A variety of macromolecules including cationic lipids,¹ polylysine,² polyethylenimine,³ and dendrimers⁴ have been used as carriers to bind to negatively charged plasmid DNA and facilitate spontaneous gene transfer in cell culture as a result of charge interaction between the DNA carrier complex and the cell surface. Unfortunately, the performance of these nonviral gene delivery carriers are far less efficient *in vivo* due in part to the rapid pharmacokinetics and clearance of DNA complexes.^{5,6} This relates to both the particle size and surface charge of the delivery system.⁷ For example, cationic lipids form large DNA complexes that are trapped in the capillary beds of the lung⁵ whereas smaller (<100 nm) peptide DNA condensates are scavenged by mononuclear phagocytic system (MPS) cells of the liver,⁶ limiting the development of DNA delivery systems that target peripheral tissues.

The intravenous dosing of most colloids leads to opsonization and MPS cell uptake in the lung, liver, and spleen.⁸ In the case of liposomes, this limitation has been largely overcome by simultaneously reducing the particle size to <100 nm and modifying the surface with PEG⁹ since

this polymer possesses the ideal hydration and flexibility to create a steric layer that allows liposomes to avoid opsonization and detection by MPS cells.¹⁰

Several studies have described the synthesis of PEG-containing polymers designed to create a steric layer on the surface of DNA condensates,^{7,11–17} with the aim of improving their solubility and *in vivo* performance. An early study by Wolfert et al. described the synthesis of grafted copolymers of PEG (5 or 12 kDa) and polylysine₁₀₀ prepared by carbodiimide coupling 5–10 mol % of succinylated-PEG onto the side chains of polylysine.^{11,12} The resulting PEG-peptides were less toxic to cells in culture compared to polylysine₁₀₀, formed DNA condensates possessing a reduced effective surface charge, and had slightly improved solubility over control polylysine DNA condensates but surprisingly were unable to reduce spontaneous gene transfer in HepG2 cells¹² *in vitro*, suggesting that they would not be able to block nonspecific interactions with cells *in vivo*.

Subsequently, Choi et al. derivatized the side chains of polylysine₁₂₀ with 5–25 mol % low molecular weight PEG of 550 Da.¹³ The resulting PEG-peptide DNA condensates were also less toxic to cells than polylysine₁₂₀ DNA condensates but were similar to Wolfert's PEG-peptides in their inability to reduce spontaneous gene transfer in HepG2 cells, indicating that low molecular weight PEG was no more effective than high molecular weight PEG. Using a similar approach, PEG polylysine dendrimer copolymers were recently reported by the same group and used to form DNA condensates that were more nuclease resistant than polylysine DNA condensates but which were not examined for gene transfer.¹⁴

In addition, Katayose et al. synthesized PEG-polylysine block copolymers to incorporate 5 kDa PEG into polylysine by random polymerization of *N*-carboxyanhydride ε-(benzyloxycarbonyl)-lysine with amino-PEG, resulting in a polymer with a lysine to PEG ratio of approximately 18:1^{15,16} representing approximately 5 mol % PEG. These PEG-polylysine DNA condensates were also reportedly much more resistant to endonuclease than uncondensed DNA but were not examined for solubility or gene transfer.^{16,17}

To date, there are no reports of a PEG-peptide DNA condensing agents that significantly increase the solubility of the DNA condensates and/or reduce spontaneous gene transfer to HepG2 cells. These are both significant problems since the poor solubility of peptide DNA condensates of approximately 50–100 μg/mL limits the dosing volume and precludes dose escalation during *in vivo* gene transfer. Likewise, reducing the level of spontaneous gene transfer *in vitro* is a first step toward developing DNA formulations that avoid nonspecific gene transfer to cells *in vivo* and may allow the development of DNA formulations that target to peripheral sites. Here we describe the synthesis and formulation properties of two PEG-peptides, both of which

* To whom correspondence should be addressed. Tel: 734-763-1032. Fax: 734-763-2022. E-mail: krice@umich.edu.

significantly improve DNA condensate solubility and one of which dramatically reduces spontaneous gene transfer of DNA condensates *in vitro*. The results suggest that these two properties are closely linked to the loading level of PEG on peptide DNA condensates.

Materials and Methods

PEG-orthopyridyl disulfide (PEG-OPSS, 5 kDa) and PEG-vinyl sulfone (PEG-VS, 5 kDa) were purchased from Shearwater Inc. (Huntsville, AL) and Fluka (Ronkonkoma, NY), respectively. Fetal calf serum and LipofectAce were obtained from Gibco BRL (Gaithersburg, MD). Minimum essential media (MEM) and CM Sephadex C50 were purchased from Sigma (St. Louis, MO). TCEP (tris(2-carboxyethyl)phosphine hydrochloride) was purchased from Aldrich, (Milwaukee, WI). D-Luciferin and luciferase from *Photinus pyralis* were from Boehringer Mannheim (Indianapolis, IN). The 5.6 kb plasmid (pCMVL) encoding the reporter gene luciferase under the control of the cytomegalovirus promoter was a gift from Dr. M. A. Hickman at the University of California, Davis.¹⁸ pCMVL was produced in *E. coli* and purified using a Qiagen Ultrapure-100 kit (Santa Clarita, CA). Bradford reagent was purchased from Bio-Rad (Hercules, CA). Preparative and analytical C18 reverse phase HPLC columns were purchased from Vydac (Hesperia, CA). HPLC was performed using a computer-interfaced HPLC and fraction collector from ISCO (Lincoln, NE).

Synthesis of PEG-VS-CWK₁₈ and PEG-SS-CWK₁₈—CWK₁₈ (Cys-Trp-Lys)₁₈ and dimeric-CWK₁₈ were synthesized and characterized as described previously.¹⁹ The Cys residue on CWK₁₈ was alkylated with iodoacetic acid resulting in AlkCWK₁₈ as reported.¹⁹ The synthesis of PEG-VS-CWK₁₈ utilized dimeric-CWK₁₈ (0.5 μ mol) which was reduced to form 1 μ mol of CWK₁₈ by reaction with 25 μ mol of TCEP²⁰ in 0.5 mL of 0.1 M sodium phosphate pH 7 for 4 h at room temperature. PEG-VS-CWK₁₈ was formed by reacting 1 μ mol of reduced CWK₁₈ with 30 μ mol of PEG-VS in a total volume of 1.2 mL of 0.1 M sodium phosphate pH 7 at room temperature for 12 h. The progress of the reaction was monitored by analytical RP-HPLC eluted at 1 mL/min with 0.1% TFA and a gradient of acetonitrile (5–65% over 30 min) while detecting by $A_{280\text{nm}}$. The reaction mixture was applied to a CM Sephadex C50 cation-exchange column (0.7 \times 15 cm) eluted with 60 mL of water to remove free PEG-VS as the unbound fraction and then with 15 mL of 1.5 M sodium chloride while collecting 5 mL fractions. PEG-VS-CWK₁₈ and CWK₁₈ were detected by $A_{280\text{nm}}$ and were pooled and desalted by 5 h dialysis against 4 L of water in 1000 MWCO tubing and then freeze-dried. PEG-VS-CWK₁₈ was resolved from CWK₁₈ by injecting 0.5 μ mol onto a semipreparative C18 RP-HPLC column (2 \times 25 cm) eluted at 10 mL/min with 0.1% TFA and a gradient of acetonitrile (5 to 65% over 30 min) while detecting by $A_{280\text{nm}}$. The peak eluting at 25 min yielded 0.8 μ mol of PEG-VS-CWK₁₈ (80%) based on tryptophan absorbance ($\epsilon_{280\text{nm}} = 5600 \text{ M}^{-1} \text{ cm}^{-1}$).

A disulfide bond exchange reaction was used to prepare PEG-SS-CWK₁₈. Prior to conjugation of PEG-OPSS, dimeric-CWK₁₈ was reduced and then purified by RP-HPLC eluted as described above. Reduced CWK₁₈ (1 μ mol) was reacted with 4 μ mol of PEG-OPSS in 1 mL of 0.1 M sodium phosphate pH 7 at room temperature for 30 min. The reaction was monitored by analytical RP-HPLC which detected a single new product peak eluting at 25 min. PEG-SS-CWK₁₈ was purified by injecting 0.5 μ mol portions onto semipreparative RP-HPLC eluted as described above resulting in an isolated yield of 95%.

PEG-VS-CWK₁₈ and PEG-SS-CWK₁₈ (1 μ mol) were prepared for ¹H NMR by D₂O exchange followed by dissolving the sample in 0.5 mL of D₂O (99.96%) containing acetone as an internal standard. ¹H NMR spectra were generated on a Bruker 500 MHz spectrometer operated at 23 °C. PEG-peptides were prepared for MALDI-TOF by dissolving 5 nmol in 20 μ L of water. These (0.5 μ L) were combined with 0.5 μ L of saturated α -cyano-4-hydroxycinnamic acid in 50 v/v % acetonitrile and 0.3% trifluoroacetic acid and then analyzed on a Vestec LaserTec MS (PerSeptive Biosystems, Framingham, MA) operated in the linear mode at 20 kV.

Formulation of Peptide DNA Condensates—Peptide DNA condensates were formed by adding 75 μ g of DNA (pCMVL in 750 μ L of 5 mM Hepes pH 7.4) to varying amounts of peptide (7.5 to 90 nmol in 750 μ L of Hepes) while vortexing, followed by equilibration at room temperature for 1 h. Peptide binding to DNA

was monitored by a fluorescent dye displacement assay.¹⁹ A 1 μ g aliquot of the peptide DNA condensate was diluted to 1 mL in Hepes containing 0.1 μ M thiazole orange. The fluorescence of the intercalated dye was measured on an LS50B fluorometer (Perkin-Elmer, UK) in a microcuvette by exciting at 500 nm while monitoring emission at 530 nm.

The particle size of peptide DNA condensates were analyzed at a DNA concentration of 50 μ g/mL in Hepes by quasielastic light scattering (QELS). The particle surface charge was determined by ζ (zeta) potential analysis using a Brookhaven ZetaPlus (Brookhaven Instruments). The solubility of peptide DNA condensates were determined by measuring particle size as a function of DNA concentration (50 μ g/mL to 2 mg/mL) at a constant peptide: DNA stoichiometry of 0.4 nmol of peptide per μ g of DNA corresponding to a charge ratio ($\text{NH}_4^+:\text{PO}_4^-$) of 2.3:1.

DNA cocondensates were prepared by add-mixing AlkCWK₁₈ and PEG-VS-CWK₁₈ in ratios ranging from 0 to 100 mol % and condensing DNA at a charge ratio of 2.3:1 as described above. To establish the mol ratio of peptides bound to DNA, condensates were dialyzed in a fixed volume (0.5 mL) dialyzer for 75 h against water using a 100 000 MWCO membrane. Peptide DNA condensates in the retentate (0.5 mL) were dissociated by adding 50 μ L of 5 M sodium chloride in 0.1% TFA. AlkCWK₁₈ and PEG-VS-CWK₁₈ were quantified by injecting 1 nmol of peptide (100 μ L) onto analytical RP-HPLC eluted with 0.1% TFA and a gradient of acetonitrile (5 to 65% over 30 min) while detecting tryptophan by fluorescence ($\lambda_{\text{ex}280\text{nm}}$, $\lambda_{\text{em}350\text{nm}}$). The peak integration areas were used to quantify AlkCWK₁₈ and PEG-VS-CWK₁₈ with reference to standard curves developed for each peptide.

In Vitro Gene Expression and Cell Binding—HepG2 cells were plated at 1.5×10^5 cells per 35 mm well and grown to 40–70% confluence in MEM supplemented with 10% fetal calf serum (FCS). Peptide DNA condensates (10 μ g of DNA) were added dropwise to triplicate sets of cells in 2% FCS containing 80 μ M chloroquine. After 5 h incubation at 37 °C, the media was replaced with MEM supplemented with 10% FCS, and luciferase expression was determined at 24 h. Cells were washed twice with ice-cold phosphate-buffered saline (calcium and magnesium free) and then treated with 0.5 mL of ice-cold lysis buffer (25 mM Tris hydrochloride pH 7.8, 1 mM EDTA, 8 mM magnesium chloride, 1% Triton X-100, 1 mM DTT) for 10 min. The cell lysate was scraped, transferred to 1.5 mL microcentrifuge tubes, and centrifuged for 7 min at 13 000g at 4 °C to pellet debris. Lysis buffer (300 μ L), sodium-ATP (4 μ L of a 180 mM solution, pH 7, 4 °C), and cell lysate (100 μ L, 4 °C) were combined in a test tube, briefly mixed, and immediately placed in the luminometer. Luciferase relative light units (RLU) were recorded on a Lumat LB 9501 (Berthold Systems, Germany) with 10 s integration after automatic injection of 100 μ L of 0.5 mM D-luciferin (prepared fresh in lysis buffer without DTT). The expression level of luciferase was normalized for protein using the Bradford assay,²¹ and the relative light units were converted to fmol of luciferase/mg of protein using a standard curve developed by adding luciferase to cell supernatant. Each experimental result represents the mean and standard deviation derived from a triplicate set of transfections.

LipofectAce (Gibco BRL, 1:2.5 w/w dimethyl dioctadecylammonium bromide and dioleoylphosphatidylethanolamine) was optimized for use to mediate gene transfection in HepG2 cells according to the manufacturer's instructions. DNA/LipofectAce complexes were prepared by combining 10 μ g of DNA in 100 μ L of serum free media (SFM) with 60 μ L of LipofectAce prepared in 150 μ L of SFM. The LipofectAce DNA complex was then diluted with 1.7 mL of SFM and used to transfect HepG2 cells for 5 h followed by replacement of the transfecting media with MEM supplemented with 10% FBS. The cells were incubated for a total of 24 h, harvested, and then analyzed for luciferase as described above.

Iodinated plasmid DNA was prepared with specific activity of 300 nCi per μ g of DNA as described previously.²² Prior to forming DNA condensates, the specific activity of the ¹²⁵I DNA was adjusted to 4.5 nCi per μ g of DNA by combining with unlabeled plasmid. DNA condensates were prepared using AlkCWK₁₈, PEG-SS-CWK₁₈, or PEG-VS-CWK₁₈ as described above. Peptide ¹²⁵I-DNA condensates (10 μ g) were used to transfect HepG2 cells for 5 h according to the procedure described above. The radioactive media was removed, cells were washed with phosphate-buffered saline, harvested with lysis buffer, and the cell-associated radioactivity was quantified by gamma counting.

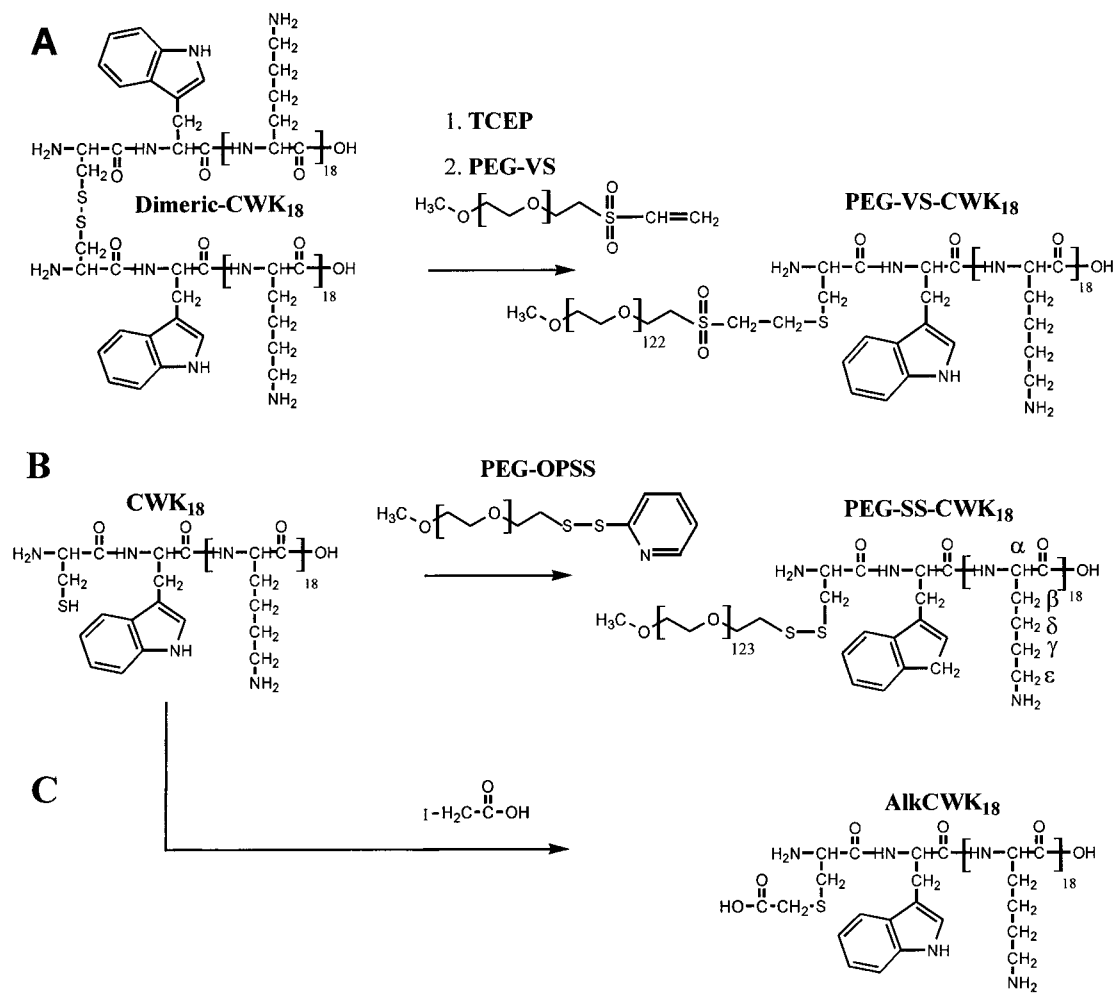


Figure 1—Reaction schemes for the synthesis of PEG-CWK₁₈ conjugates. (A) TCEP was used to reduce dimeric-CWK₁₈ to generate CWK₁₈. This was reacted in situ with PEG-VS to form PEG-VS-CWK₁₈. (B) Alternatively, the reaction of CWK₁₈ with PEG-OPSS formed PEG-SS-CWK₁₈. (C) AikCWK₁₈ was produced by reacting CWK₁₈ with iodoacetic acid. The α , β , γ , δ , and ϵ protons of Lys of PEG-SS-CWK₁₈ illustrate the nomenclature used for assigning PEG-peptides in Figure 3.

Results

PEG-Peptide Synthesis—PEG was covalently attached to the Cys residue of a 20 amino acid synthetic peptide (CWK₁₈) to prepare two PEG-peptides possessing either a reversible (PEG-SS-CWK₁₈) or irreversible (PEG-VS-CWK₁₈) covalent linkage (Figure 1). Each reaction was optimized by systematically changing the pH and the stoichiometry of peptide to PEG while monitoring the product formation by analytical RP-HPLC. Since the reaction of CWK₁₈ with PEG-VS at pH 7 was slow (12 h), TCEP was added to reduce dimeric-CWK₁₈ and also inhibit its re-formation during conjugation with PEG-VS. At pH 7, a mol ratio of PEG-VS: CWK₁₈ of 30:1 resulted in optimal conjugation to form PEG-VS-CWK₁₈. At suboptimal stoichiometries or lower pH the reaction was incomplete whereas at a higher pH, dimeric-CWK₁₈ re-formed as the major product.

In contrast to the synthesis of PEG-VS-CWK₁₈, the optimal reaction conditions to prepare PEG-SS-CWK₁₈ only required a 4 mol excess of PEG-OPSS over CWK₁₈ at pH 7. In this case, attempts to block the formation of dimeric-CWK₁₈ with TCEP led to the reduction of PEG-OPSS, completely inhibiting the desired reaction. Instead, reduced CWK₁₈ was prepared and found to react rapidly (30 min) with PEG-OPSS with minimal formation of dimeric-CWK₁₈.

RP-HPLC analysis of the crude reaction product of PEG-VS-CWK₁₈ demonstrated a nearly complete disappearance of CWK₁₈ with the formation of a new peak eluting at 25

min (Figure 2B). Despite the apparent complete resolution of the desired product, careful examination revealed that PEG-VS coeluted with PEG-VS-CWK₁₈. This was evident from NMR analysis which determined a 10-fold excess of PEG relative to CWK₁₈ in the HPLC purified product (data not shown). Consequently, PEG-VS-CWK₁₈ was purified using cation exchange to remove excess PEG-VS and then by RP-HPLC to remove unreacted CWK₁₈ resulting in a product that rechromatographed as a single peak on RP-HPLC (Figure 2D). Proton NMR analysis identified resonances assigned to the α , β , γ , δ , and ϵ protons of the Lys residues as well as the Trp aromatic resonances (Figure 3A). Integration of protons at 3.67 ppm (PEG) relative to the signal at 2.97 ppm (Lys ϵ) produced a peak area ratio of 13.5:1 corresponding to a 1:1 conjugate of PEG₁₂₂ and CWK₁₈.

RP-HPLC analysis of the crude reaction product of PEG-OPSS and CWK₁₈ identified a product peak eluting at 25 min, a PEG-OPSS reagent peak at 28 min, a thiol pyridine (TP) byproduct peak at 5 min, and a trace of dimeric-CWK₁₈ eluting at 15 min (Figure 2C). PEG-SS-CWK₁₈ was isolated in a single step by semipreparative RP-HPLC, rechromatographed as a single peak on analytical HPLC (Figure 2E), and produced an NMR spectrum with an integration ratio of PEG:Lys also establishing a 1:1 conjugate of PEG₁₂₃ and CWK₁₈ (Figure 3B).

MALDI-TOF analysis of PEG-VS-CWK₁₈ and PEG-SS-CWK₁₈ produced a broad peak centered at 8433 and 8297

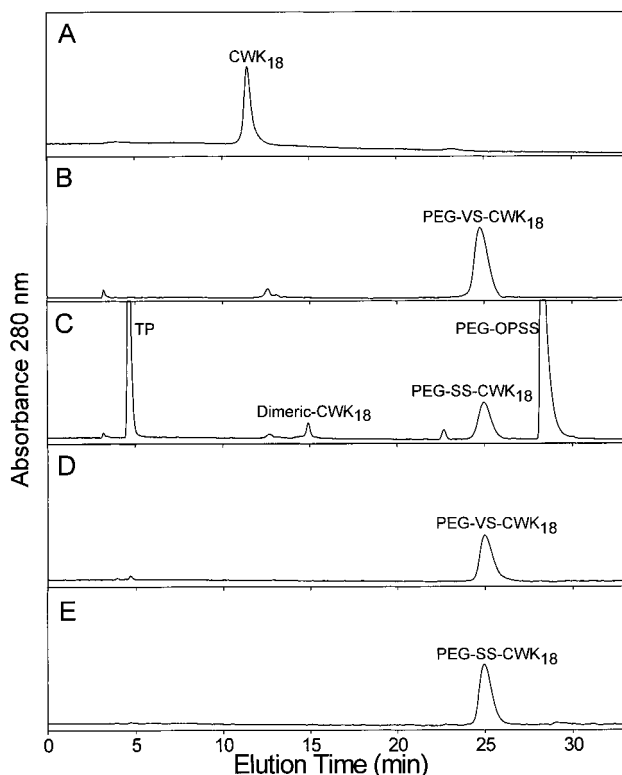


Figure 2—Analytical RP-HPLC analysis of PEG-CWK₁₈ conjugates. The reaction of dimeric-CWK₁₈ with TCEP and PEG-VS formed a single major product as shown in panel B. Alternatively, reduced CWK₁₈ (panel A) reacted with PEG-OPSS to produce PEG-SS-CWK₁₈, dimeric-CWK₁₈, thiol-pyridine (TP), and unreacted PEG-OPSS as shown in panel C. Purified PEG-VS-CWK₁₈ and PEG-SS-CWK₁₈ both eluted as a single peak as shown in panels D and E, respectively.

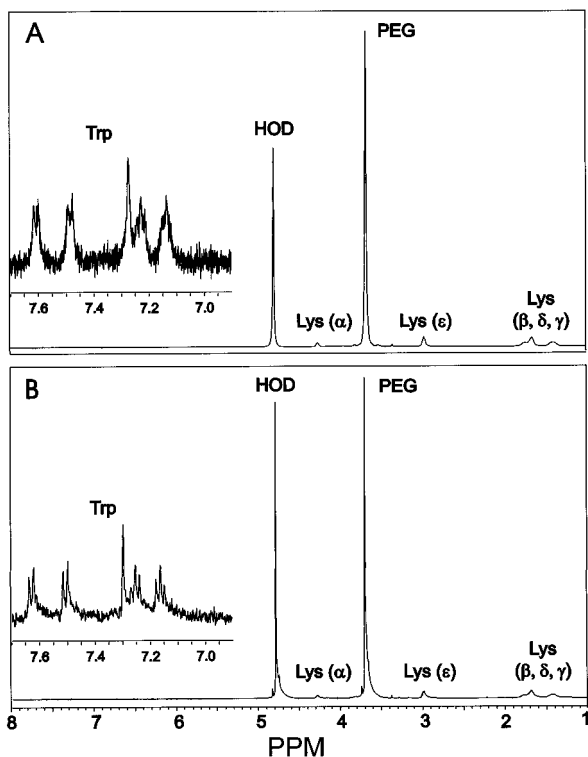


Figure 3—¹H NMR analysis of PEG-CWK₁₈ conjugates. The 500 MHz ¹H NMR spectrum of PEG-VS-CWK₁₈ (panel A) and PEG-SS-CWK₁₈ (panel B) are illustrated with the key signals of the Lys, Trp and PEG identified according to Figure 1. The integration of the ε protons of Lys relative to the PEG protons established a degree of polymerization of 122 for PEG-VS-CWK₁₈ and 123 for PEG-SS-CWK₁₈.

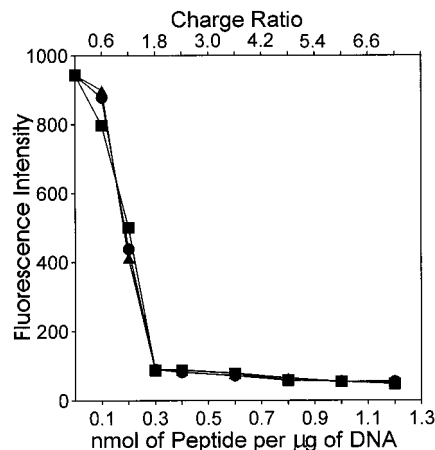


Figure 4—Relative binding affinity of PEG-CWK₁₈ conjugates to DNA. The fluorescence intensity resulting from the titration of AlkCWK₁₈ (●), PEG-SS-CWK₁₈ (■), and PEG-VS-CWK₁₈ (▲) to compete for intercalator dye binding to DNA is shown. An asymptote at 0.3 nmol of each peptide per μg of DNA established that each peptide binds to DNA with equivalent affinity.

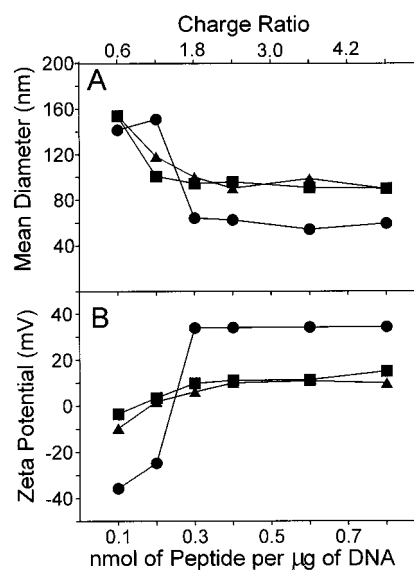


Figure 5—QELS particle size and ζ potential analysis of PEG-CWK₁₈ DNA condensates. The mean particle size of AlkCWK₁₈ (●), PEG-SS-CWK₁₈ (■), and PEG-VS-CWK₁₈ (▲) DNA condensates is plotted as a function of peptide:DNA stoichiometry in panel A. The mean ζ potential for each DNA condensate is plotted in panel B. An indistinguishable particle size and ζ potential was determined for each PEG-CWK₁₈ conjugate. However, a significant decrease in the ζ potential for PEG-CWK₁₈ DNA condensates (+10 mV) versus AlkCWK₁₈ DNA condensates (+35 mV) provided evidence of the formation of a steric barrier.

m/z, respectively. These results were consistent with the formation of conjugates of CWK₁₈ (2648 amu) and polydisperse PEG of approximately 5800 Da.

PEG-Peptide DNA Condensate Formulation—The DNA binding affinity of AlkCWK₁₈, PEG-VS-CWK₁₈, and PEG-SS-CWK₁₈ were compared using a fluorescent dye displacement assay. A coincident titration curve for each peptide with an asymptote at 0.3 nmol per μg of DNA corresponding to a charge ratio of 1.8:1 suggested that both PEG-peptides bind to DNA with equivalent affinity as AlkCWK₁₈ (Figure 4).

The particle size and ζ potential of DNA condensates prepared with AlkCWK₁₈, PEG-VS-CWK₁₈, and PEG-SS-CWK₁₈ were examined as a function of peptide:DNA stoichiometry (Figure 5). The mean diameter for both PEG-peptide DNA condensates was 90 nm at a charge ratio of 1.8:1 or higher whereas the mean diameter for AlkCWK₁₈

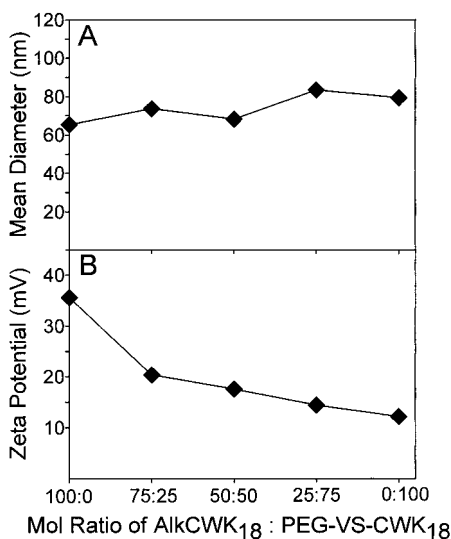


Figure 6—QELS particle size and ζ potential analysis of peptide DNA cocondensates. Particle size analysis was used to characterize peptide DNA cocondensates prepared at 50 $\mu\text{g}/\text{mL}$ of DNA and varying mol % of AlkCWK₁₈ and PEG-VS-CWK₁₈ as shown in panel A. The ζ potential of DNA cocondensates is shown in panel B. The mean particle size changes from 65 to 80 nm whereas the ζ potential of DNA cocondensates decreases from +35 to +10 mV with increasing mol % of PEG-VS-CWK₁₈.

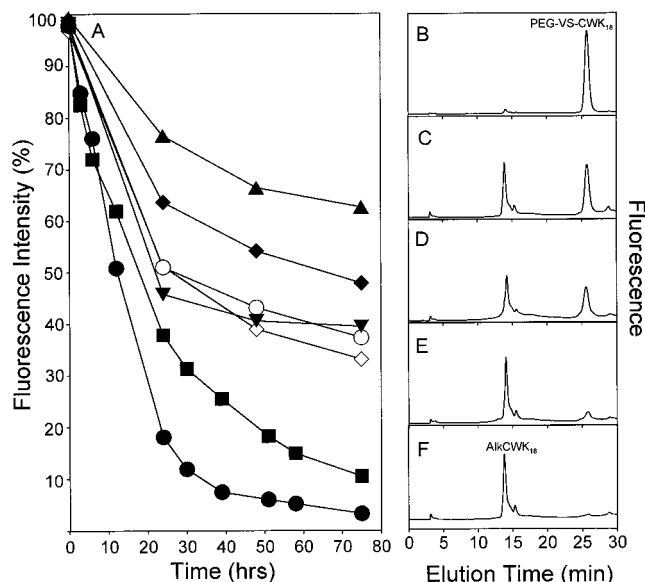


Figure 7—RP-HPLC analysis of peptide DNA cocondensates. The time course of dialysis of free AlkCWK₁₈ (●), free PEG-VS-CWK₁₈ (■), AlkCWK₁₈ DNA condensates (▼), PEG-VS-CWK₁₈ DNA (▲), and cocondensates of 25:75 (◆), 50:50 (○), 75:25 (◇) mol % of AlkCWK₁₈:PEG-VS-CWK₁₈ bound to DNA was determined by tryptophan fluorescence of the retentate (panel A). After 75 h of dialysis, peptide DNA condensates in the retentate were dissociated with sodium chloride and directly chromatographed on RP-HPLC. Panels B–F illustrate chromatograms resulting from 100 mol % PEG-VS-CWK₁₈ DNA condensates (panel B), DNA cocondensates prepared with 75:25 (panel C), 50:50 (panel D), 25:75 (panel E) PEG-VS-CWK₁₈:AlkCWK₁₈, and 100 mol % AlkCWK₁₈ DNA condensates (panel F).

DNA condensates was 60 nm (Figure 5A). In contrast, a large decrease in ζ potential of +25 mV was identified for PEG-peptide DNA condensates at a charge ratio of 1.8:1 compared to AlkCWK₁₈ DNA condensates (Figure 5B).

Since PEG-VS-CWK₁₈ and AlkCWK₁₈ possess equivalent DNA binding affinity, add-mixtures of the two peptides were used to prepare DNA cocondensates. The average particle size increased from 65 to 80 nm using add-mixtures of AlkCWK₁₈ and PEG-VS-CWK₁₈ varying from 0 to 100 mol % while keeping the charge ratio constant at 2.3:1

Table 1—Quantitative Analysis of DNA Cocondensates

input add-mixture (mol % AlkCWK ₁₈ : mol % PEG-VS-CWK ₁₈)	recovery ratio ^a (mol % AlkCWK ₁₈ : mol % PEG-VS-CWK ₁₈)
0:100	0:100
25:75	41:59
50:50	59:41
75:25	82:18
100:0	100:0

^a Based on HPLC standard curves developed for AlkCWK₁₈ and PEG-VS-CWK₁₈.

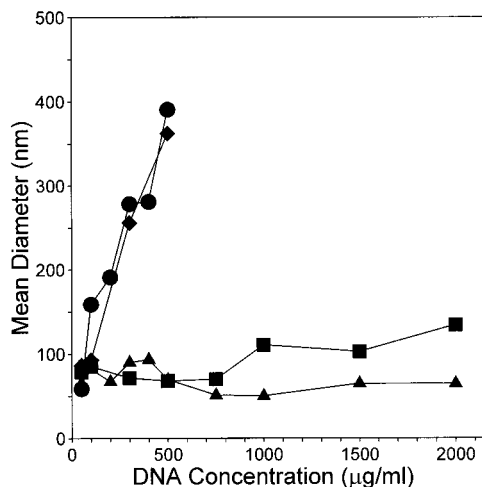


Figure 8—Solubility of peptide DNA condensates. Particle size analysis was performed as a function of DNA concentration using 100 mol % AlkCWK₁₈ (●) and 100 mol % PEG-VS-CWK₁₈ (▲) DNA condensates and using AlkCWK₁₈:PEG-VS-CWK₁₈ DNA cocondensates prepared with 50 (◆) and 90 (■) mol % PEG-VS-CWK₁₈. The particle size increased to >400 nm above 500 $\mu\text{g}/\text{mL}$ for AlkCWK₁₈ DNA condensates but remained at <100 nm for PEG-VS-CWK₁₈ DNA condensates throughout concentrations up to 2 mg/mL.

(Figure 6A). Likewise, the ζ potential decreased from +35 mV to +10 mV as the stoichiometry of PEG-VS-CWK₁₈ increased (Figure 6B), suggesting the formation of DNA cocondensates with intermediate PEG loading.

To further confirm the formation of DNA cocondensates, unbound peptides were removed by microdialysis and the ratio of peptides bound to DNA was determined by HPLC. Control experiments established the nearly complete removal (>90%) of free AlkCWK₁₈ or PEG-VS-CWK₁₈ from the retentate after 75 h of dialysis (Figure 7A). However, the dialysis of DNA cocondensates prepared at charge ratios of 2.3:1 resulted in the removal of unbound peptide and retention of >35% of the tryptophan fluorescence. Dissociation and RP-HPLC analysis of the retained peptide (Figure 7B–F) allowed recovery of AlkCWK₁₈ and PEG-VS-CWK₁₈ at ratios that agreed to within 16% of the input ratio for each DNA cocondensate (Table 1) in which the loss of PEG-VS-CWK₁₈ was greater than that of AlkCWK₁₈.

DNA condensate solubility was evaluated by examining the particle size of concentrated solutions. AlkCWK₁₈ DNA condensates increased in particle size from 60 to 400 nm when increasing DNA concentration from 50 to 500 $\mu\text{g}/\text{mL}$ and then formed visible flocculates at higher concentrations. Alternatively, PEG-VS-CWK₁₈ DNA condensates maintained a mean diameter of <100 nm throughout concentrations ranging from 0.05 to 2 mg/mL and showed no sign of increasing in size (Figure 8). Likewise, substitution of PEG-SS-CWK₁₈ for PEG-VS-CWK₁₈ resulted in the formation of DNA condensates with 88 nm mean diameter at 2 mg/mL.

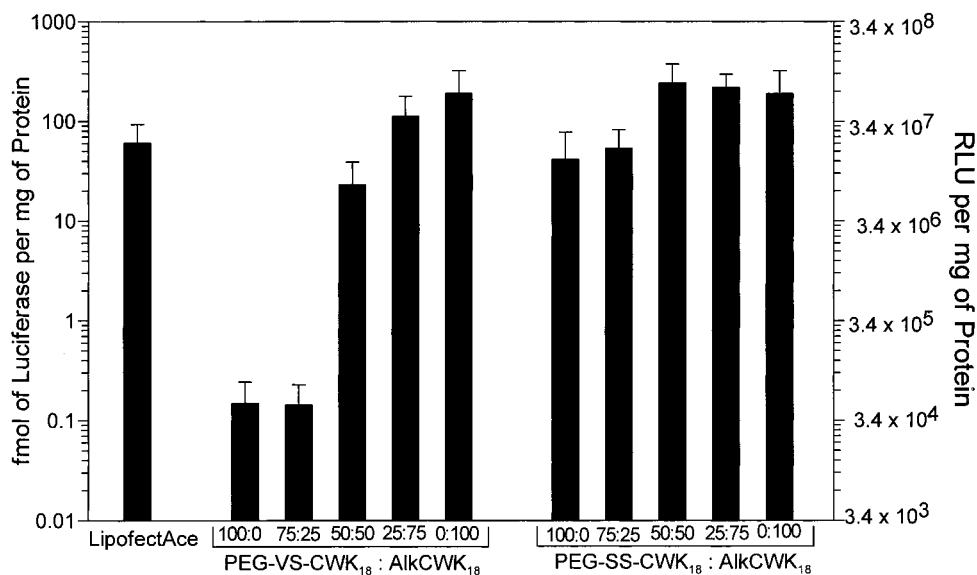


Figure 9—In vitro gene transfer efficiency of PEG-CWK₁₈ DNA condensates. The in vitro expression of luciferase in HepG2 cells is compared for PEG-VS-CWK₁₈ and PEG-SS-CWK₁₈ as well as cocondensates prepared with AlkCWK₁₈ at the ratios indicated. LipofectAce is included as a control gene transfer agent.

DNA cocondensates containing 50 mol % PEG-VS-CWK₁₈ and AlkCWK₁₈ possessed similar poor solubility properties to that of 100 mol % AlkCWK₁₈ DNA condensates. However, DNA cocondensates composed of 90 mol % PEG-VS-CWK₁₈ and 10 mol % AlkCWK₁₈ also maintained a particle size of <100 nm up to 750 μg/mL and then formed larger particles (>100 nm) at DNA concentrations of 1 mg/mL or higher (Figure 8).

DNA condensates prepared with PEG-VS-CWK₁₈, PEG-SS-CWK₁₈, AlkCWK₁₈, and add-mixtures of AlkCWK₁₈ and PEG-peptides were compared by measuring luciferase expression in HepG2 cells 24 h post-transfection (Figure 9). PEG-VS-CWK₁₈ DNA condensates reduced spontaneous gene transfer by three orders of magnitude compared to AlkCWK₁₈ DNA condensates. The reduction was only 10-fold when transfecting with DNA cocondensates prepared with 50 mol % PEG-VS-CWK₁₈ and only 2-fold using cocondensates composed of 25 mol % PEG-VS-CWK₁₈ (Figure 9).

The gene transfer properties of PEG-SS-CWK₁₈ DNA condensates were significantly different than PEG-VS-CWK₁₈ DNA condensates. DNA condensates prepared with 100 or 75 mol % PEG-SS-CWK₁₈ reduced spontaneous gene transfer by 5-fold relative to AlkCWK₁₈ DNA condensates while DNA cocondensates prepared with 50 or 25 mol % of PEG-SS-CWK₁₈ were equivalent to AlkCWK₁₈ DNA condensates (Figure 9).

The cell binding of ¹²⁵I-DNA was compared for AlkCWK₁₈, PEG-VS-CWK₁₈, and PEG-SS-CWK₁₈ DNA condensates during a 5 h transfection. Approximately 14% of the radioactivity was cell-associated for AlkCWK₁₈ DNA condensates whereas only 6.8% and 0.2% were cell-associated when using PEG-SS-CWK₁₈ and PEG-VS-CWK₁₈ as DNA condensing agents, respectively (Figure 10). These results correlated well with the observed gene transfer efficiency for each peptide DNA condensate, suggesting differences in the uptake of these condensates was the main cause of their difference in gene expression.

Discussion

The targeting of DNA to specific cells in vivo for the purpose of mediating therapeutically relevant levels of gene expression will require systematic optimization of the drug delivery system.²³ The design of such delivery systems must

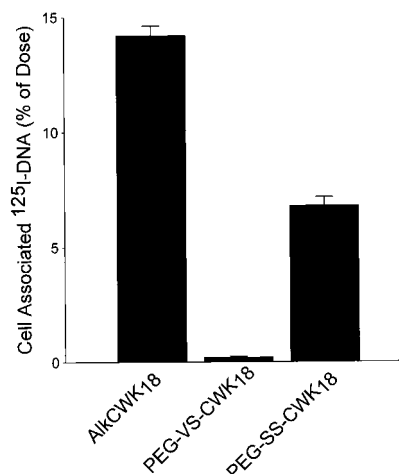


Figure 10—HepG2 cell binding of peptide DNA condensates. HepG2 cells were transfected for 5 h with 45 nCi (10 μg) of ¹²⁵I-DNA condensates prepared with either AlkCWK₁₈, PEG-VS-CWK₁₈, or PEG-SS-CWK₁₈. The cell associated DNA recovered is expressed as the percent of ¹²⁵I-DNA dosed onto cells. The results represent the mean ± SD for three determinations.

attempt to minimize the carrier's toxicity and antigenicity, increase the DNA's metabolic stability, control the particle size and charge, and increase the DNA condensate solubility as well as provide a means to target DNA to the nucleus of the cell. Thus far, PEG-peptides have been reported to decrease toxicity,^{11–13} increase DNA stability,^{14,17} and improve DNA solubility.¹² In the present study we report the synthesis of two PEG-peptides that simultaneously create very soluble DNA condensates and significantly inhibit spontaneous gene transfer of peptide DNA condensates in vitro. A major finding is that both of these properties are influenced to different degrees by the load level of PEG on DNA condensates.

The directed synthesis of the low molecular weight PEG-peptides reported here is a major distinction of this work compared to others. The conjugation of PEG (5000 Da) to a single cysteine of CWK₁₈ afforded highly purified PEG-peptides that controlled the PEG attachment site and allowed comparison of reducible and nonreducible linkages. Notably, the apparent binding affinity of both PEG-peptides for DNA were equivalent to AlkCWK₁₈ as determined by the intercalator exclusion assay (Figure 4),

indicating that conjugates of CWK₁₈ retain their ability to bind and condense DNA. Due to the homogeneity of the peptide portion of PEG-VS-CWK₁₈ and PEG-SS-CWK₁₈, DNA condensates formed at charge ratios of 1.8:1 or higher achieved a constant particle size and ζ potential, establishing both the absence of interfering peptides and that excess PEG-peptide does not bind to fully condensed DNA.

ζ potential measurements revealed evidence that PEG-peptides altered the surface properties of DNA condensate. The ζ potential of PEG-VS-CWK₁₈ and PEG-SS-CWK₁₈ DNA condensates were indistinguishable and reached a minimum of +10 mV at a calculated charge ratio of 1.8:1 (Figure 5B). The decrease in ζ potential resulted from the covalent attachment of PEG since the addition of equivalent amounts of free PEG to AlkCWK₁₈ DNA condensates did not influence its ζ potential (data not shown). Likewise, analysis of DNA cocondensates established a correlation between the ζ potential and the mol % of PEG-VS-CWK₁₈ incorporated into the cocondensate (Figure 6B). The recovery of the approximate input ratio of AlkCWK₁₈ and PEG-VS-CWK₁₈ following prolonged dialysis confirmed the formation of DNA cocondensates. This allowed add-mixing of two condensing peptides (AlkCWK₁₈ and PEG-VS-CWK₁₈) to systematically alter both physical and biological properties of peptide DNA condensates.

The formation of a steric layer is highly dependent on the amount PEG loaded onto DNA condensates.^{10,12} This is most evident with DNA cocondensates possessing between 0 and 25 mol % PEG-peptide where the ζ potential decreased sharply to +20 mV and then only declined gradually to reach +10 mV at 25–100 mol % PEG-peptide. Even though the ζ potential only changed by +10 mV when titrating between 25 and 100 mol % of PEG-peptide (Figure 6B), these DNA condensates were most altered in solubility and gene transfer efficiency.

The solubility achieved for 100 mol % PEG-peptide DNA condensates (2 mg/mL) is far greater than the solubility reported (60 μ g/mL) for other PEG-peptides DNA condensates.¹² This physical property appears to be very dependent on the loading density of PEG since cocondensates prepared with 50 mol % PEG-VS-CWK₁₈ were not improved in solubility relative to AlkCWK₁₈ DNA condensates. Even cocondensates formed with as much as 90 mol % PEG-VS-CWK₁₈ demonstrated an increase in particle size at concentrations greater than 750 μ g/mL, indicating that even slightly less PEG on the DNA condensate will result in lower solubility.

Earlier studies demonstrated that the in vitro gene transfer efficiency for peptide DNA condensates was dependent on the charge ratio.^{19,24} The expression reached a maximum when AlkCWK₁₈ DNA condensates were formed at charge ratio of 1.8:1 or higher, suggesting that the positive charge on DNA condensates contributes to their spontaneous transfection in cell culture. In support of this hypothesis, fully condensed PEG-VS-CWK₁₈ DNA condensates prepared at a charge ratio of 2.3:1 possess a lower ζ potential of +10 mV and reduced spontaneous gene transfer by 1000-fold compared to AlkCWK₁₈ DNA condensates. Likewise, DNA cocondensates possessing intermediate ζ potential partially reduced gene transfer, further demonstrating a correlation between DNA condensate charge and the level of spontaneous gene transfer. However, these data also established that the PEG load level needed to block spontaneous gene transfer in vitro is much lower than that required to create soluble PEG-peptide DNA condensates.

Even though PEG-VS-CWK₁₈ and PEG-SS-CWK₁₈ DNA condensates were equivalent in their physical properties, they proved to be unequal in their ability to reduce spontaneous gene transfer (Figure 9). Since the two peptides only differ in their linkage between PEG and peptide,

a possible explanation was the reduction of PEG-SS-CWK₁₈ either outside or inside the cell to form CWK₁₈ DNA condensates during the time of transfection. To test this hypothesis, radioiodinated DNA condensates were used to determine the percent cell associated after a 5 h transfection (Figure 10). PEG-VS-CWK₁₈ DNA condensates did not significantly bind to cells, with only 0.2% of the dose being cell associated. In contrast, 14% of AlkCWK₁₈ DNA condensates and 6.8% of PEG-SS-CWK₁₈ DNA condensates dose were cell-associated following 5 h transfection, supporting the hypothesis that differences in cell uptake are responsible for the 2 orders of magnitude difference in gene expression mediated by PEG-SS-CWK₁₈ and PEG-VS-CWK₁₈ DNA condensates. To determine if PEG-SS-CWK₁₈ underwent reduction during gene transfer, its stability was analyzed while incubating in cell culture media containing 2% FCS. This led to its partial reduction over time (data not shown), suggesting that the removal of PEG by disulfide bond scission results in the formation of CWK₁₈ DNA condensates in situ and is a likely explanation of the difference between PEG-SS-CWK₁₈ and PEG-VS-CWK₁₈ DNA condensates.

Therefore, the utility of PEG-SS-CWK₁₈ may be in generating soluble DNA condensates that can be formulated within a gene-activated matrix intended for implantation in which targeting is not necessary and spontaneous transfection of infiltrating cells is desired.²⁵ Alternatively, the greater stability of PEG-VS-CWK₁₈ may result in its utility in modifying the surface of DNA condensates used during intravenous gene delivery.

Future studies will demonstrate the utility of PEG-peptides in gene activated matrixes and in altering the biodistribution of DNA condensates in vivo. The ability to form DNA cocondensates that incorporate both PEG and targeting ligands attached to CWK₁₈ may provide a unique approach to systematically optimize gene delivery formulations for maximum efficacy in vivo.

References and Notes

1. Zhang, Y. P.; Reimer, D. L.; Zhang, G.; Lee, P. H.; Bally, M. B. Self-Assembling DNA-Lipid Particles for Gene Transfer. *Pharm. Res.* **1997**, *14*, 190–196.
2. Wu, G. Y.; Wu, C. H. Evidence for Targeted Gene Delivery to HepG2 Hepatoma Cells in Vitro. *Biochemistry* **1988**, *27*, 887–892.
3. Ogris, M.; Steinlein, P.; Kurs, M.; Mechtler, K.; Kirchheis, R.; Wagner, E. The Size of DNA/Transferrin-PEI complexes is an Important Factor for Gene Expression in Cultured Cells. *Gene Ther.* **1998**, *5*, 1425–1433.
4. Tang, M. X.; Redemann, C. T.; Szoka, F. C., Jr. In Vitro Gene Delivery by Degraded Polyamidoamine Dendrimers. *Bioconjugate Chem.* **1996**, *7*, 703–714.
5. Niven, R.; Pearlman, T.; Wedeking, T.; Mackeigan, J.; Noker, P.; Simpson-Herren, L.; Smith, J. G. Biodistribution of Radiolabeled Lipid-DNA Complexes and DNA in Mice. *J. Pharm. Sci.* **1996**, *87*, 1292–1299.
6. Nishikawa, M.; Takemura, S.; Takakura, Y.; Hashida, M. Targeted Delivery of Plasmid DNA to Hepatocytes In Vivo: Optimization of the Pharmacokinetics of Plasmid DNA/Galactosylated Poly (L-Lysine) Complexes by Controlling their Physicochemical Properties. *J. Pharm. Exp. Ther.* **1998**, *287*, 408–415.
7. Kwok, D. Y.; Coffin, C. C.; Lollo, C. P.; Jovenal, J.; Bananszczyk, M. G.; Mullen, P.; Phillips, A.; Amini, A.; Fabrycki, J.; Bartholomew, R. M.; Brostoff, S. W.; Carlo, D. J. Stabilization of Poly-L-Lysine/DNA Polyplexes for In Vivo Gene Delivery to the Liver. *Biochim. Biophys. Acta* **1999**, *1444*, 171–190.
8. Woodle, M. C. Controlling Liposome Blood Clearance by Surface-Grafted Polymers. *Adv. Drug Delivery Rev.* **1998**, *32*, 139–152.
9. Torchilin, V.; Omelyanenko, V. G.; Papisov, M. I.; Bogdanov, A. A.; Trubetskoy, V. S.; Herron, J. N.; Gentry, C. A. Poly(ethylene glycol) on the Liposome Surface: On the Mechanism of Polymer-Coated Liposome Longevity. *Biochim. Biophys. Acta* **1994**, *1195*, 11–20.

10. Torchilin, V. P. Polymer-Coated Long-Circulating Microparticulate Pharmaceuticals. *J. Microencaps.* **1998**, *15* (1), 1–19.
11. Wolfert, M. A.; Schacht, E. H.; Toncheva, V.; Ulbrich, K.; Nazarova, O.; Seymour, L. W. Characterization of Vectors for Gene Therapy Formed by Self-Assembly of DNA with Synthetic Block Co-Polymers. *Human Gene Ther.* **1996**, *7*, 2123–2133.
12. Toncheva, V.; Wolfert, M. A.; Dash, P. R.; Oupicky, D.; Ulbrich, K.; Seymour, L. W.; Schacht, E. H. Novel Vectors for Gene Delivery Formed by Self-Assembly of DNA with Poly(L-lysine) Grafted with Hydrophobic Polymers. *Biochim. Biophys. Acta* **1998**, *1380*, 354–368.
13. Choi, Y. H.; Liu, F.; Kim, J. K.; Choi, Y. K.; Park, J. S.; Kim, S. W. Polyethylene Glycol-Grafted Poly-L-Lysine as Polymeric Gene Carrier. *J. Controlled Release* **1998**, *54*, 39–48.
14. Choi, J. S.; Lee, E. J.; Choi, Y. H.; Jeong, J. Y.; Park, J. S. Poly(ethylene glycol)-*block*-poly(L-lysine) Dendrimer: Novel Linear Polymer/Dendrimer Block Copolymer Forming a Spherical Water-Soluble Polyionic Complex with DNA. *Bioconjugate Chem.* **1999**, *10*, 62–65.
15. Harada, A.; Kataoka, K. Formation of Polyion Complex Micelles in an Aqueous Milieu from a Pair of Oppositely-Charged Block Copolymers with Poly(ethylene glycol) Segments. *Macromolecules* **1995**, *28*, 5294–5299.
16. Katayose, S.; Kataoka, K. Water-Soluble Polyion Complex Associates of DNA and Poly(ethylene glycol)-Poly(L-lysine) Block Copolymers. *Bioconjugate Chem.* **1997**, *8*, 702–707.
17. Katayose, S.; Kataoka, K. Remarkable Increase in Nuclease Resistance of Plasmid Supramolecular Assembly with Poly(ethylene glycol)-Poly(L-lysine) Block Copolymer. *J. Pharm. Sci.* **1998**, *87*, 160–163.
18. Plank, C.; Zatloukal, K.; Cotten, M.; Mechtler, K.; Wagner, E. Gene Transfer into Hepatocytes Using Asialoglycoprotein Receptor Mediated Endocytosis of DNA Complexed with an Artificial Tetraantennary Galactose Ligand. *Bioconjugate Chem.* **1992**, *3*, 533–539.
19. Wadhwa, M. S.; Collard, W. T.; Adami, R. C.; McKenzie, D. L.; Rice, K. G. Peptide-Mediated Gene Delivery: Influence of Peptide Structure on Gene Expression. *Bioconjugate Chem.* **1997**, *8*, 81–88.
20. Burns, J. A.; Butler, J. C.; Moran, J.; Whitesides, G. M. Selective Reduction of Disulfides by Tris-(2-carboxyethyl)-phosphine. *J. Org. Chem.* **1991**, *56*, 2648–2650.
21. Bradford, M. M. A Rapid and Sensitive Method for the Quantitation of Microgram Quantities of Protein Utilizing the Principle of Protein-Dye Binding. *Anal. Biochem.* **1976**, *72*, 248–254.
22. Teribesi, J.; Kwok, K. Y.; Rice, K. G. Iodinated Plasmid DNA as a Tool for Studying Gene Delivery. *Anal. Biochem.* **1998**, *263*, 120–123.
23. Pouton, C. W.; Seymour, L. W. Key Issues in Non-Viral Gene Delivery. *Adv. Drug Delivery Rev.* **1998**, *34*, 3–19.
24. Wadhwa, M. S.; Knoell, D.; Young, T.; Rice, K. G. Targeted Gene Delivery with a Low Molecular Weight Glycopeptide. *Bioconjugate Chem.* **1995**, *6*, 283–291.
25. Fang, J.; Zhu, Y. Y.; Smiley, E.; Bonadio, J.; Rouleau, J.; Goldstein, S. A.; McCauley, L. K.; Davidson, B. L.; Roessler, B. J. Stimulation of New Bone Formation by Direct Transfer of Osteogenic Plasmid Genes. *Proc. Natl. Acad. Sci.* **1996**, *93*, 5753–5758.

Acknowledgments

The authors acknowledge financial support provided by NIH grants GM48049, DE13004 and support from Selective Genetics, Inc.

JS990072S